Research Article

Novel Microfluidic Design and Lab-on-a-Disc Adaptation for Efficient Hematocrit Screening at the Population Level

Santi Rattanavarin* and Thanapat Sangkharat*
Department of Production and Robotics Engineering, Faculty of Engineering, King Mongkut's University of Technology North Bangkok, Bangkok, Thailand

Ekachai Juntasaro
Mechanical Engineering Simulation and Design Group, Mechanical and Automotive Engineering Program, The Sirindhorn International Thai-German Graduate School of Engineering, King Mongkut's University of Technology North Bangkok, Bangkok, Thailand

Witsaroot Sripumkhai, Pattaraluck Pattamang and Wutthinan Jeamsaksiri
Thai Microelectronics Center, National Science and Technology Development Agency, Chachoengsao, Thailand

Numfon Khemthongcharoen, Ratthasart Amarit, Sataporn Chanhorm and Pongsakun Sripetch
Photonics Technology Research Team, National Electronics and Computer Technology Center, National Science and Technology Development Agency, Pathum Thani, Thailand

Kamonchanok Duangkanya
Terahertz Technology Research Team, National Electronics and Computer Technology Center, National Science and Technology Development Agency, Pathum Thani, Thailand

Chompunoot Sinthupibulyakit
Faculty of Medical Technology, Huachiew Chalermprakiet University, Samut Prakan, Thailand

* Corresponding author. E-mail: santi.rattanavarin@email.kmutnb.ac.th DOI: 10.14416/j.asep.2026.04.005
Received: 8 July 2025; Revised: 12 September 2025; Accepted: 26 January 2026; Published online: 8 April 2026

Abstract
Hematocrit (Hct) measurement is a crucial diagnostic parameter for evaluating oxygen transport capacity and detecting anemia or polycythemia. Conventional microhematocrit methods, while widely used, have limitations, including the requirement for relatively large blood volumes, fragile glass capillary tubes, manual sample handling, and reliance on high-speed centrifugation, restricting their practicality in point-of-care testing (POCT). Lab-on-a-disc (LoD) centrifugal microfluidic platforms have emerged as promising POCT solutions, offering automation and efficiency in blood analysis. However, most existing designs incorporate multiple microfluidic channels and sample inlets on a single disc, making them impractical for single-use applications. This study presents a novel, single-use microfluidic-based blood collection device integrated with a LoD system for efficient and minimally invasive hematocrit screening. The device requires only 5 µL of blood and utilizes capillary action for self-filling, eliminating the need for wax sealing. The optimized microfluidic design enables low-speed centrifugation (7,000 rpm for 5 min) while maintaining high accuracy ($R^2 = 0.9996$) compared to the standard method. An automated image-processing system ensures precise hematocrit measurement, while QR integration enhances sample identification and data management, making this system ideal for large-scale screening. The compact and lightweight design makes it highly suitable for mobile healthcare screening units, enabling rapid, safe, and cost-effective hematocrit assessment in remote and resource-limited settings. This proposed method significantly advances accessibility and efficiency in population health monitoring.

Keywords: Anemia, Blood collection device, Centrifugal microfluidic, Hematocrit screening, Lab-on-a-disc

1 Introduction

Hematocrit (HCT) is the proportion of red blood cells (RBCs) in the total blood volume and serves as a key indicator of the blood's ability to transport oxygen and carbon dioxide [1]. Abnormal hematocrit levels can compromise this function and are associated with various clinical conditions. Low hematocrit, indicative of anemia, results in reduced oxygen delivery to tissues and may cause symptoms such as fatigue, pallor, dizziness, shortness of breath, and weakness. Common causes include blood loss, nutritional deficiencies (iron, vitamin B12, folate), chronic diseases, autoimmune disorders, and bone marrow suppression [2], [3]. High hematocrit reflects increased RBC mass or decreased plasma volume and may lead to increased blood viscosity, raising the risk of thrombosis and cardiovascular complications. Causes include dehydration, polycythemia vera, chronic hypoxia, and elevated erythropoietin levels [4]–[7]. Elevated hematocrit is also frequently observed in neonates, especially those born preterm, due to physiological and developmental factors [8].

The National Committee for Clinical Laboratory Standards (NCCLS) recommends hematocrit determination by centrifugation as the reference method. In this microhematocrit technique, a small blood sample is collected into a glass capillary tube, one end is sealed with wax, and the sample is centrifuged at 12,000 rpm for 5 minutes. Hematocrit is calculated by measuring the proportion of packed red blood cells to the total blood volume, expressed as a percentage [9]. This method requires only a minimal sample, typically obtained via skin prick from the fingertip or heel, and is widely used due to its safety, simplicity, and low cost. It is particularly suited for anemia screening in blood donors and high–risk populations [10], [11]. Anemia remains a major global health concern, affecting roughly one–third of the population [12]–[14]. It is especially common among vulnerable groups such as children aged 6–59 months, school–aged children, pregnant women, and women of reproductive age (15–49 years) [15]–[17]. Global estimates report anemia prevalence as 42% in children under five, 25.4% in school–aged children, and 30% in women of reproductive age [13], [15], [18]. Iron deficiency, often due to inadequate dietary intake, accounts for approximately 60% of anemia cases [19]. Regular hematocrit screening is recommended by the World Health Organization (WHO) and the U.S. Preventive Services Task Force (USPSTF) as an important tool for early anemia diagnosis and management. Early detection is critical for initiating timely interventions and preventing complications, particularly in at–risk populations [1], [11]

The microhematocrit method is a straightforward diagnostic tool that provides several benefits for use in large–scale surveys and screening programs. However, it is associated with notable limitations that can impact its practicality and efficiency. Firstly, the method requires a relatively large blood volume (50–60 μl) [3], which can be particularly inconvenient in scenarios where minimal invasiveness is preferred, such as in pediatric patients, preterm infants, or when multiple daily sample collections are needed for treatment monitoring. The method relies on fragile glass capillary tubes that are prone to breaking during handling or high-speed centrifugation, posing safety risks to medical staff and leading to potential sample loss. Additionally, the open end of the capillary tube must be sealed with wax after blood collection. This step introduces the potential for human error and operational inefficiencies, as leakage of the wax seal can frequently result in sample loss. Reading the hematocrit ratio is often performed manually using a graphical reading device, making the accuracy of measurements highly dependent on the skill of the technician [20].

Conventional hematocrit (Hct) measurement methods involve manual sample labeling and handling, making them time–consuming and susceptible to errors, particularly in large–scale screening programs. These methods also require high–speed centrifugation (~12,000 rpm), necessitating bulky laboratory equipment that is unsuitable for point–of–care testing (POCT). Additionally, the lack of automation reduces efficiency, making the process labor–intensive and subject to variability. Lab–on–Disc (LoD) centrifugal microfluidic platforms have emerged as a promising alternative for rapid blood cells and plasma separation in POCT applications [21]–[24]. Previous studies have demonstrated LoD systems capable of complete blood count (CBC) analysis, including Hct measurement of a whole blood sample [25]. However, many of these systems rely on complex microfluidic designs with integrated fluorescent imaging, which are challenging to scale for industrial manufacturing. Several simplified LoD designs for Hct measurement have been investigated. For example, a polyester–toner disc with U–shaped channels enabled simultaneous analysis of 12 finger–prick samples on the same disc using an imaging–based readout [26]. Another design incorporated a metering channel with a downstream blind channel for

air–bubble priming, allowing straightforward visual inspection of Hct. This configuration, fabricated in a compact disc (CD) format, accommodated up to 9 samples introduced by pipetting [27]. A different strategy integrated siphon valves at varying levels of the main channel to facilitate Hct estimation without manual measurement of fluid height, with up to 4 samples analyzed per disc [28]. More recently, a dead–end microfluidic platform used centrifugal force and hydraulic resistance for self–filling of nanoliter–scale blood samples, enabling Hct and white blood cell quantification simultaneously [29]. While LoD technologies offer clear advantages in automation, portability, and efficiency, most existing designs feature multiple channels and sample inlets, limiting their feasibility for single–use applications. In our previous work, we introduced a simplified single–use LoD–based Hct measuring device using a hand–pumping mechanism for precise blood collection [30]. However, the technique differs from the conventional capillary–based blood collection methods routinely used by medical staff, potentially limiting its adoption in clinical settings.

This study introduces a novel single–use, LoD–based system for blood collection and hematocrit measurement that addresses key limitations of conventional methods. The device requires only 5 µl of blood, providing a minimally invasive and practical solution for point–of–care testing. Its microfluidic design enables efficient red cell packing under low–speed centrifugation, allowing for a smaller, lower–cost, and portable centrifugal unit. A closed–end microfluidic design eliminates the need for waxing, simplifying sample preparation. The device is made of durable plastic, making it unbreakable compared to traditional microcapillary glass tubes, thereby reducing sample loss and improving operator safety. Furthermore, the device includes a designated area for QR code or patient ID labeling, streamlining population screening tests by reducing labeling errors and ensuring compatibility with the automated hematocrit measurement system for the population's digital records. Collectively, these features offer a safe, user–friendly, and cost–effective approach to hematocrit testing in both clinical and population–based settings.

2 Materials and Methods

2.1 *Design and fabrication of the blood collection device*

The blood collection device developed in this study is designed to minimize pain, reduce the need for excessive finger squeezing, and enhance usability for healthcare providers. It enables the collection of an adequate blood sample within 20 seconds from a single drop using the smallest commercially available safety lancet (30G, 1.2–1.5 mm depth), which typically yields 18–32 µL of blood [31]. This rapid sampling improves both safety and efficiency, and the shallow puncture reduces pain, making it especially suitable for pediatric and preterm infants. The device measures 45 × 18 × 1.10 mm (L × W × H) and consists of three layers. The top and bottom layers are fabricated from polymethyl methacrylate (PMMA) sheets, while the intermediate layer consists of a microchannel structure produced from an adhesive transfer tape (3M; 467 MP). The tape comprises a polyethylene terephthalate (PET) sheet coated on both sides with a pressure-sensitive adhesive (PSA). Prior to assembly, PMMA layers were cleaned with detergent, rinsed with deionized water, and dried with compressed air. Layer alignment was performed using a pin-based alignment system, followed by compression at 10 kg/cm² for 2 minutes using a hydraulic press to ensure robust structural integrity. The device's composition and structure are shown in Figure 1.

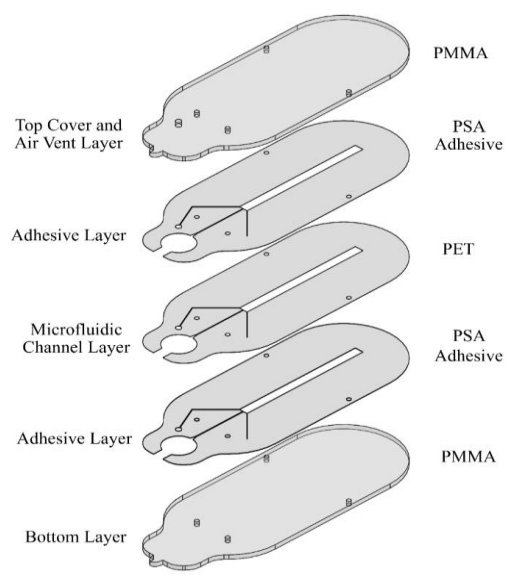

Figure 1: Exploded view of the microfluidic blood collection device showing its multilayer structure: a PMMA top cover, a PET–based microfluidic channel layer with double–sided PSA coatings, and a PMMA bottom substrate. Alignment pinholes ensure precise lamination, while a through–hole air vent across all layers facilitates passive flow and pressure balance.

This multilayer configuration enables well–defined microchannel geometries, improves mechanical stability, and provides robust sealing.

Figure 2 demonstrates the design of the blood collection device, which comprises a sample inlet, a sample collection chamber, an air vent channel, and a hematocrit measurement chamber. The sampling volume of the device is determined by the cylindrical dimensions of the sample collection chamber, with a depth of 0.22 ± 0.02 mm and a radius of 2.6 ± 0.1 mm, resulting in an estimated sample volume of 4.57 ± 0.93 µL. Before using the devices in subsequent experiments, all devices were treated with air plasma at a power of 50 watts for 30 seconds to enhance surface energy at the inlet tip. The blood sample can be spontaneously drawn into the sample collection chamber by capillary action within the fluidic channel.

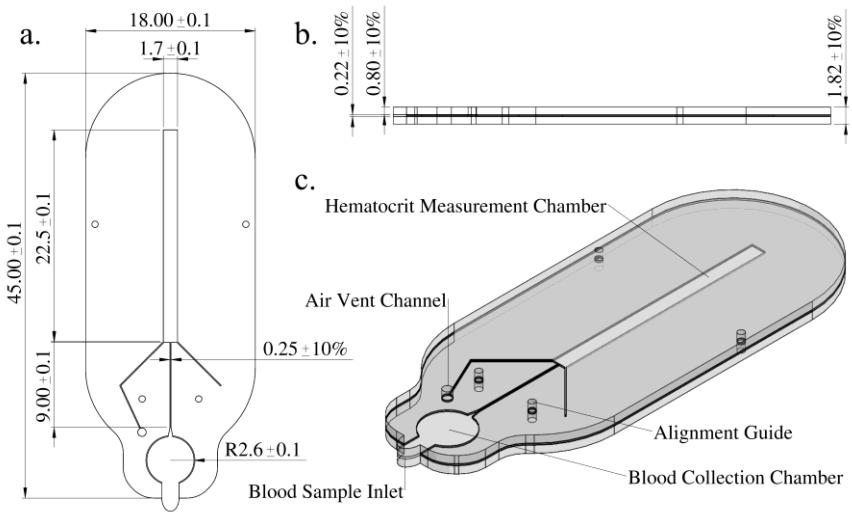

Figure 2: Design and dimensions of the blood collection device. (a) Top view showing the overall length (45.0±0.1 mm), width (18.0±0.1 mm), hematocrit measurement chamber width (1.7±0.1 mm), and flow–resistant channel width (0.25±10%). (b) Side view illustrating the total device thickness (1.82±10%) and channel height (0.22±10%). (c) Three–dimensional schematic highlighting the major functional components, including the blood sample inlet, blood sample collection chamber, hematocrit measurement chamber, air vent channel, and alignment guide.

During sample collection, the device is gently brought into contact with a blood drop on the fingertip, allowing the sample to be drawn into the collection chamber via capillary action. Once inside the chamber, the blood spontaneously advances into the microfluidic channel, which is positioned between two open ends: the sample inlet and an air vent. The movement of the liquid within the channel is governed by the interplay between the upward capillary force (F_{upward}) and the opposing gravitational force ($F_{downward}$) [32], [33], as illustrated in Figure 3. Capillary forces dominate in the narrow microchannel, enabling passive blood transport without the need for external pumps or equipment. The open–ended design ensures continuous air displacement, facilitating smooth fluid flow and preventing backpressure buildup.

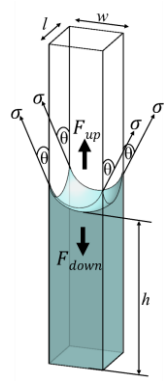

Figure 3: Schematic illustrating liquid movement in the microfluidic channel, governed by the balance between upward capillary force (F_{upward}) and downward gravitational force ($F_{downward}$).

When the contact angle θ between the liquid and the solid surface is considered, the vertical component of the capillary force responsible for liquid rise can be determined based on classical capillarity theory. The pressure–driven force acting along the liquid–solid interface can be resolved into vertical and horizontal components depending on the contact angle θ, with the vertical component contributing to liquid rise being proportional to $\cos\theta$. Accordingly, the upward force can be expressed as Equation (1) [34]:

$$F_{upward} = \sigma P \cos\theta \quad (1)$$

where σ is the surface tension coefficient of blood (53.45 mN/m) [35], P is the perimeter of the rectangular cross–section (which varies with distance from the inlet tip of the microfluidic channel), and θ is the contact angle between blood and the well–cleaned PMMA surface (64°, as determined experimentally). For a rectangular channel with width (w) and length (l), the perimeter is defined as P = 2(w + l). In this device, width (w) represents the thickness of the microfluidic channel, which is 220 µm.

The opposing gravitational force arising from the weight of the liquid column can be derived from the classical hydrostatic pressure relationship $F_{downward} = PA$, where the force exerted by a fluid at rest on a surface equals the product of pressure and area. The hydrostatic pressure P is given by $P = \rho g h$, where ρ is the fluid density, g is the gravitational acceleration, and h is the height of the liquid column. Accordingly, the total downward force acting on the surface of area A at depth h is expressed as Equation (2) [34]:

$$F_{downward} = \rho g A h \quad (2)$$

where ρ is the density of blood (1,060 kg/m^3) [36], g is gravitational acceleration (9.8 m/s^2), h is the height of the blood column measured from the inlet tip, and A = w × l is the cross-sectional area. The channel thickness (w) is fixed at 220 µm.

In the proposed microfluidic device, both the capillary force (F_{upward}) and the gravitational force due to the liquid weight ($F_{downward}$) vary with height from the sample inlet tip, as they are influenced by the changing channel length (l) and the cumulative liquid volume. The relationship between F_{upward} and $F_{downward}$ as a function of height is represented graphically in Figure 4.

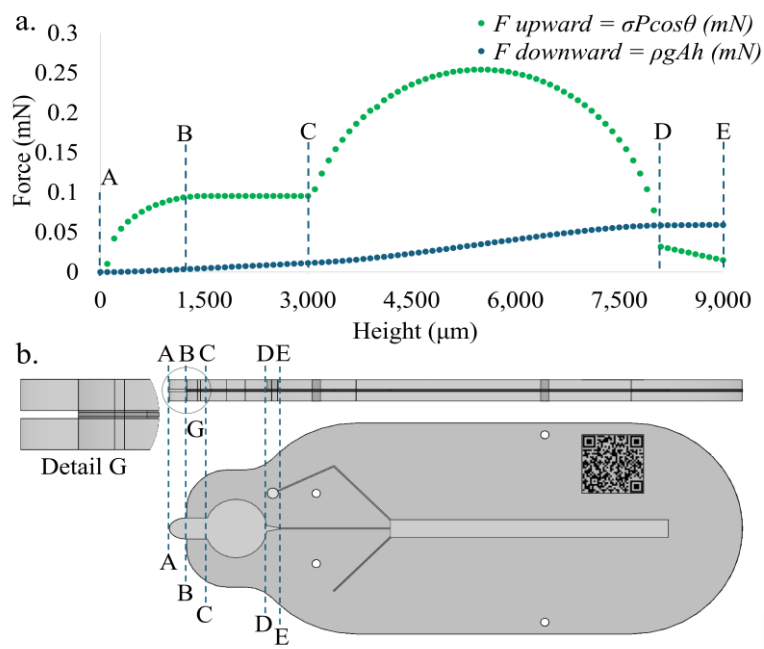

Figure 4: (a) plot of capillary force (green, F = σPcosθ) and gravitational force (blue, F = ρgAh) as functions of fluid height from the inlet tip of the microfluidic chip. (b) Schematic cross–section of the chip showing the fluid pathway, with dashed lines (A–E) marking positions that correlate structural changes in the channel with force variations in the graph.

2.2 *Blood sample preparation*

Blood samples used in the experiments were collected and prepared under an optimal protocol approved by the IRB committee (No. ๑.1251/2565, Huachiew Chalermprakiet University).

2.3 *Precision of the sample volume collection*

The sample collection chamber in the microfluidic design determines the device's ability to control the collected sample volume. Once the chamber is completely filled through spontaneous capillary action, further sample flow is restricted by a narrow, flow–resistant channel. This design ensures consistent sample volume collection for each examination. To evaluate the accuracy and precision of sample volume collection, 137 devices were weighed before and after blood sample collection. The mean, standard deviation (SD), and coefficient of variation (CV) of the collected blood weight were calculated to assess the consistency and reliability of the device in controlling sample volume.

2.4 *Optimization of the centrifugal speed for hematocrit measurement*

To prepare a packed red cell for hematocrit (Hct) measurement using the blood collection device, a custom device holder was fabricated to function as a rotor adapter for a mini–centrifuge (Daihan Scientific; CF-10), as shown in Figure 5.

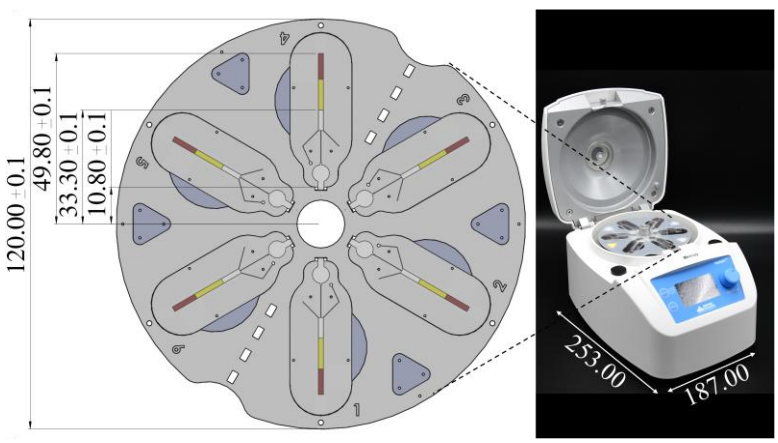

Figure 5: Design of the centrifugal holder and portable centrifuge used in the experiments: (left) custom rotor accommodating up to six microfluidic devices (120 mm diameter) with marked radial distances from the centrifugal center to the bottom of the tube (49.8 ± 0.1 mm), sample surface (33.3 ± 0.1 mm), and inlet tip (10.8 ± 0.1 mm), used for calculating optimal speed; (right) photograph of the compact benchtop centrifuge (253 × 187 mm) with the customized rotor installed.

Given the dimensional specification of both the blood collection device and the centrifuge holder, the required centrifugal speed for achieving complete red cell packing for Hct measurement can be determined using the cell pelleting Equation (3), as described below [37].

$$t = \frac{9\eta}{2\omega^2 R^2\left(\rho_p - \rho_{m)}\right)} \frac{1}{(1-C)^p} \ln\left(\frac{r_2}{r_1}\right) \quad (3)$$

In the cell pelleting equation, t represents the centrifugal time, η denotes whole blood viscosity, ω is the centrifugation speed, and R is the centrifugal radius. The densities of red blood cells and whole blood are represented by ρ_p and ρ_m, respectively. The packed red cell fraction is indicated by C, while r refers to the radial distance from the center of rotation to the bottom of the microfluidic tube (r_2) and to the sample surface (r_1). By assigning a centrifugation time of 5 min, equivalent to the duration used in the standard hematocrit measurement method, the required centrifugation speed (ω) for complete red cell packing in the microfluidic device was determined to be 6,760 rpm. Additionally, the effects of varying centrifugation speeds and durations on the packed red cell ratio within the blood collection device were systematically investigated, with the results presented in Figure 10.

2.5 *Repeatability and reliability of the microfluidic device for Hct measurement*

This study was conducted to evaluate system performance during the design and development phase. A repeatability test requires at least 20–30 repeated measurements on the same sample to obtain a statistically meaningful estimate of measurement variability, as recommended in ISO 5725-2 Accuracy (trueness and precision) of measurement methods and CLSI EP05-A3 Evaluation of Precision of Quantitative Measurement Procedures. Reliability was evaluated by comparing hematocrit (Hct) values measured using the developed system with those obtained from the reference method. Given that the expected difference between two means and the SD from both methods is ≤1 and ≤0.8, respectively, statistical analysis requires at least 13 paired measurements to compare two independent means (t–test) with a 5% significance level estimated using Statulator Sample Size Calculator [38]. Accordingly, Hct measurements were evaluated using blood samples categorized into low, normal, and high Hct levels. Each sample was measured 20 times by both the microfluidic device and the reference method to assess repeatability and reliability. An automated Hct reader operated with LabView, as shown in Figure 6, was developed to measure Hct values from the microfluidic blood collection device. The mean Hct values obtained from the microfluidic-based method and the standard method were compared using a T–test. Additionally, the coefficient of variation (CV) and total error (TE) were calculated to assess the repeatability and reliability of the microfluidic–based method in accordance with the European Federation of Clinical Chemistry and Laboratory Medicine (EFLM) database and Clinical Laboratory Improvement Amendments (CLIA) guidelines.

Figure 6: Automated hematocrit (Hct) reading system with an integrated image processing module developed in the LabVIEW environment. The system comprises a custom optical detection unit (left) for capturing images of microfluidic blood collection devices positioned on the centrifugal holder, and a computer interface (right) for data visualization. The software automatically defines measurement regions, quantifies packed red cell levels, and reports Hct values for multiple samples simultaneously, enabling rapid, consistent, and reliable data acquisition.

2.6 *Method correlation*

A method correlation study was conducted to evaluate the agreement between the developed microfluidic–based method and the reference method. Based on an expected correlation coefficient greater than 0.95, at least five paired samples are required for statistical evaluation Sample Size Calculator for Correlation [39]. For this study, blood samples collected in EDTA tubes were centrifuged to separate the red cell pellet from the plasma fraction. The pellet was subsequently diluted with plasma to prepare 120 blood samples with hematocrit (Hct) levels ranging from 20% to 70%. Each sample was measured using both the standard method and the microfluidic–based method. The resulting Hct values from the two methods were plotted to generate a correlation curve, and the agreement was assessed using the coefficient of determination (R^2).

2.7 *The setup of an automated Hct reader*

An automated Hct reader consists of an image acquisition system integrated with image processing for measurement. The five main components of the setup, shown in Figure 7, include an LED module (light source with diffuser), a plate rotor (sample holder), a stepper motor (for sample positioning), a camera module (detector), and a control unit (integrating the processing system, motor controller, and display). During operation, a centrifugal holder containing six samples is placed on the plate rotor, which is positioned between the LED module and the camera module to establish the optical detection path. Driven by the motor control system, each sample is sequentially moved into the optical path. The camera, triggered by the control unit, captures the image of the corresponding sample, which is then processed by the image analysis program, and the results are displayed on the unit screen. An image processing module was developed in the LabVIEW environment using a fixed threshold approach. The camera's focal plane remained constant, as the distance between the camera and the plate rotor was fixed within the device housing. Calibration was performed using a grid

distortion model to correct lens distortion. For hematocrit (Hct) analysis, a region of interest (ROI) was defined over the dedicated measurement channel of the microfluidic device, ensuring consistent geometry of the analysis area. The gain and exposure settings were automatically controlled by LabVIEW software to regulate image brightness before analysis, thereby ensuring reproducibility and consistent performance under field conditions.

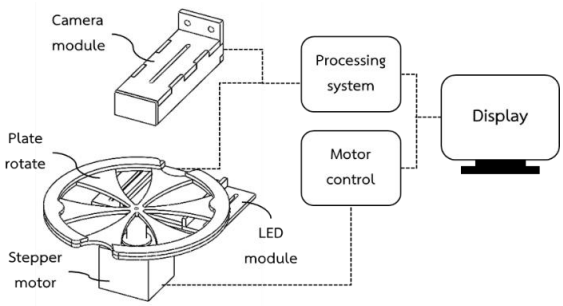

Figure 7: Image acquisition setup comprising five main components: LED module with diffuser (light source), plate rotor (sample holder), stepper motor (sample positioning), camera module (detector), and control unit integrating the processing system, motor controller, and display.

3 Results

3.1 *Precision of the sample volume collection*

Regarding the design drawing of the device shown in Figures 8a and 8b, the calculated blood volume confined within the sample inlet chamber and the sample collection chamber is 5.75 µl. Experimental evaluation using 137 devices yielded an average collected sample volume of 5.82 ± 0.36 µl, with no individual device exceeding two standard deviations (2SD) from the mean, as illustrated in Figure 8c. This result closely aligns with the designed volume, demonstrating the accuracy of the device's volume control. The coefficient of variation (CV) was determined to be 6.23%, indicating a high level of consistency in sample volume collection

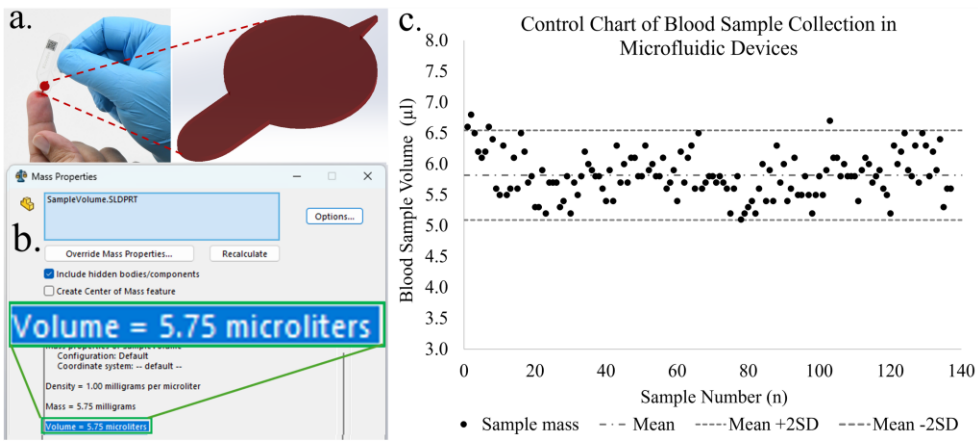

Figure 8: (a) Design of the inlet and sample collection chamber of the microfluidic device. (b) Calculated sample volume capacity determined from the 3D model, showing a theoretical capacity of 5.75 µL. (c) Control chart of blood sample uptake across 137 devices, demonstrating consistency of collected sample volume within the expected range.

3.2 *Optimization of the centrifugal speed for hematocrit measurement*

The centrifugation speed and duration were varied between 3,000 and 7,000 rpm for 3 to 5 minutes to facilitate the precipitation of red blood cells in a normal blood sample. The packed red cell formation within the portable centrifuge is demonstrated in Figure 9(a) and (b). The hematocrit (Hct) percentage, which represents the red cell packed ratio, was plotted for each centrifugation condition, as shown in Figure 9(c).

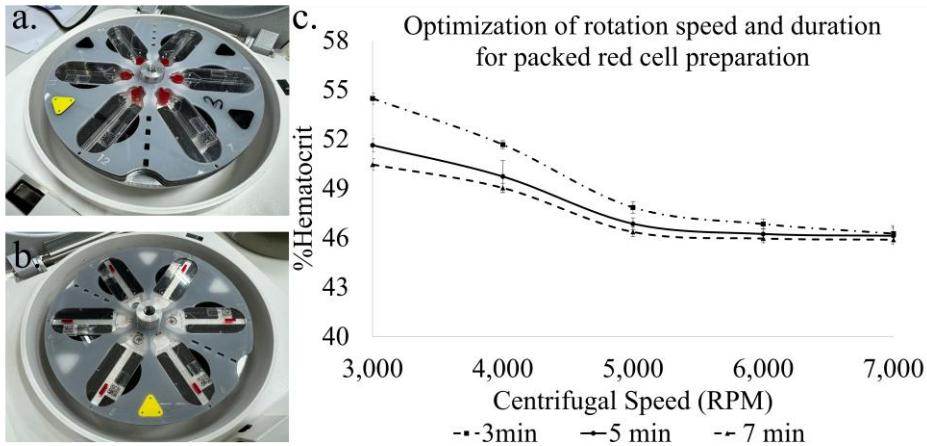

Figure 9: (a) Blood collection devices loaded in the portable centrifuge prior to centrifugation and (b) after separation of packed red cells. (c) Optimization of centrifugation speed and duration for packed red cell preparation, showing hematocrit levels as a function of centrifugal speed at 3, 5, and 7 min.

The results indicate that the packed red cell formation reached a steady level at 6,000 rpm centrifugation speed for 5 min. Based on these findings, a centrifugation speed of 7,000 rpm for 5 min was selected for further experiments.

3.3 *Repeatability and reliability of the microfluidic device for Hct measurement*

Figure 10(a) and (b) demonstrate the preparation of packed red cells for Hct measurement using two methods: centrifugation in capillary tubes at 12,000 rpm for 5 min and in the microfluidic blood collection devices at 7,000 rpm for 5 min. Blood samples with low, normal, and high Hct levels were analyzed 20 times per sample using both methods. The average Hct values obtained from the standard and microfluidic–based methods were plotted, as shown in Figure 10(c).

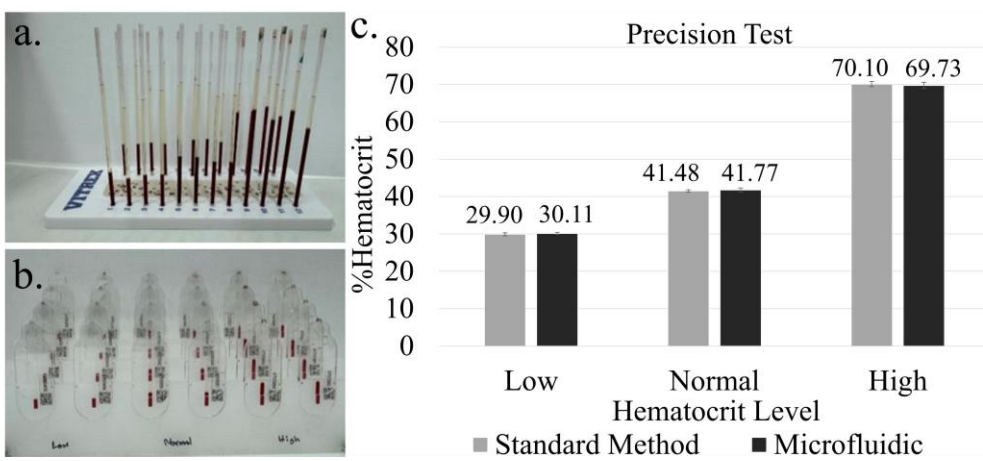

Figure 10: Packed red cell samples with low, normal, and high hematocrit (Hct) levels prepared by centrifugation in (a) standard microcapillary tubes and (b) microfluidic blood collection devices. (c) Comparison of average Hct values obtained using the standard method and the microfluidic method across the three hematocrit levels.

The mean hematocrit (Hct) values measured using the microfluidic–based method were 30.11% (CV = 0.87), 41.77% (CV = 1.24), and 69.73% (CV = 0.82) for low, normal, and high Hct samples, respectively. These coefficients of variation (CVs) fall within the expected range of biological variation reported by the EFLM [40]. Comparison with the standard method, *p*–values of 0.079, 0.082, and 0.085 for low, normal, and high samples, respectively, indicating no statistically significant differences (*p*-value > 0.05). The total error (TE) of the microfluidic method was 1.04%, 1.77%, and 2.16% for the respective Hct levels, all within the ±4% allowable error limit recommended by CLIA [41]. These results demonstrate that the microfluidic–based method offers accuracy and precision comparable to the standard technique, providing a reliable and reproducible alternative for Hct measurement.

3.4 *Method correlation*

Figure 11 presents the correlation curve of Hct measurements from 120 samples using both the standard method and microfluidic–based methods. The results show a strong linear correlation between the two methods, with a *p*–value < 0.001. The relationship between the Hct values obtained from both methods closely follows a 1:1 ratio, represented by the equation y=1.015x, with an R^2 value of 0.9996.

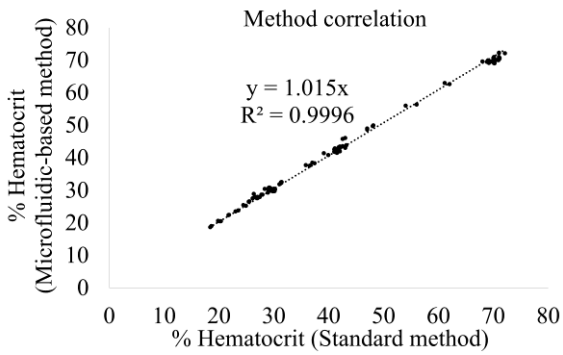

Figure 11: Correlation between hematocrit (Hct) values measured by the standard method and the microfluidic–based method after packed red cell centrifugation. The regression line demonstrates strong agreement (y = 1.015x, R^2 = 0.9996).

4 Discussion

The microfluidic collection device for hematocrit (Hct) measurement provides accurate and precise results using only 5 µL of blood, which is more than 10 times less than the volume required by standard methods. Utilizing capillary forces, the device enables self-loading without the need for pipetting tools. It is designed as a single–use, disposable unit and incorporates a QR code for individual sample identification. When used in conjunction with an automated Hct reader and cloud–based data management, the system offers a scalable solution for large–scale Hct screening.

Traditional methods for hematocrit (Hct) measurement face several limitations. These include the use of fragile glass capillary tubes, complicated procedures, and the potential for sample loss due to tube or wax seal breakage. Additionally, they rely on bulky, high–speed centrifuges, which are not suitable for point–of–care or mobile healthcare applications. Although plastic capillary tubes have been introduced to enhance durability [42], they still require high–speed centrifugation and do not substantially simplify the overall workflow. Several microfluidic-based devices have been proposed to address the challenges of conventional Hct measurement [26], [27], [43]. While these devices improve ease of operation and reduce costs, many are not designed for individual sample use, making them less suitable for clinical applications. Furthermore, they often require extra pipetting accessories, which can be impractical for point–of–care testing (POCT) and mobile healthcare units. This work proposes a novel centrifugal microfluidic platform designed for self–blood collection from fingertip or heel pricks. This device mimics the function of traditional microcapillary tubes while offering significant improvements in usability and performance. It is made from polymethyl methacrylate (PMMA), a commercially available thermoplastic widely used for its biocompatibility, safety, low toxicity, and chemical stability [44]. This new design enables hematocrit separation without the need for wax sealing. It is compatible with portable centrifuges, enhancing its suitability for decentralized and resource–limited settings. Furthermore, patient samples are identified through QR code registration, ensuring accurate identification and preventing errors associated with mislabeling. Overall, this device offers a practical, efficient, and reliable solution for Hct measurement, particularly in resource-limited and mobile healthcare settings.

This microfluidic design features an air vent located at the top corner of the hematocrit (Hct) measurement chamber. When the device is oriented with the air vent opposite the direction of centrifugal

force, the blood flows along the chamber wall away from the vent, enabling efficient centrifugation without leakage or air bubble formation. The optimal centrifugal speed for complete red blood cell (RBC) packing in this device is calculated to be 6,760 rpm over 5 minutes, substantially lower than the 11,292–12,071 rpm typically required for conventional microcapillary tubes [9]. This reduction is primarily due to the lower sample height in the microfluidic chamber, as described by the cell pelleting equation [37]. Unlike conventional methods, where sample height varies with blood volume, the microfluidic device defines a fixed sample volume through the blood collection chamber geometry. During collection, blood enters through the inlet, decelerates in a constricted channel, and is confined within the chamber. This controlled filling mechanism enhances measurement repeatability by standardizing sample volume, thereby improving the reliability and reproducibility of Hct measuring results.

The self–sampling function of the device in this study is driven by capillary action, which can be optimized by increasing the hydrophilicity of the inner surface within the microfluidic channel. In this work, air plasma treatment was used to enhance the hydrophilicity at the inlet tip of the device. To further improve the device's shelf life, future research will focus on chemically modifying the inner surface of the inlet channel to sustain and enhance its hydrophilic properties over time.

5 Conclusions

We have developed a hematocrit (Hct) measurement system that integrates a single-use microfluidic blood collection device with an automated Hct reading system. The blood collection device requires only 5 μL of blood, making it minimally invasive and well-suited for point-of-care testing. Its design enables efficient packed red cell preparation at low centrifugal speeds. Constructed from durable plastic with a closed-end structure, the device simplifies the Hct measurement process by eliminating procedural complexities associated with traditional methods. The automated Hct reader further enhances measurement consistency, reliability, and usability. Importantly, the system incorporates features that support scalability for population-level implementation. QR-code–based sample identification and cloud-based data management enable streamlined tracking, secure record integration, and real-time data sharing. These capabilities extend the applicability of the system beyond clinical settings to large-scale community screening and epidemiological studies. Taken together, this integrated approach provides a practical, reliable, and scalable solution for hematocrit testing in both clinical diagnostics and public health applications.

Acknowledgments

This work was partially supported by the Health System Research Institute (HSRI), Thailand (Grant No. HSRI. 67-054). The authors would like to express their sincere gratitude to the laboratory staff of the Faculty of Medical Technology, Huachiew University, for their kind assistance during the pre-clinical testing.

Author Contributions

S.R., T.S., E.J., N.K., W.S., P.P., and C.S.: conceptualization; S.R., T.S., E.J., and N.K.: reviewing writing an original draft and editing; S.R., T.S., E.J., W.S., P.P., W.J., N.K., R.A., S.C., P.S., K.D., and C.S.: methodology, research design, data analysis; S.R., W.S., P.P., N.K., R.A., S.C., P.S., K.D., and C.S.: experiments; S.R., N.K., W.S., and P.P.: funding acquisition, project administration. All authors have read and agreed to the published version of the manuscript.

Conflicts of Interest

The authors declare no conflict of interest.

Declaration of generative AI and AI-assisted technologies in the writing process

The authors utilized the ChatGPT tool to enhance the language and readability of the manuscript.

References

[1] H. Mondal and M. Zubair, *Hematocrit*. Treasure Island (FL): StatPearls Publishing, 2004.

[2] L. Quintó et al., "Relationship between haemoglobin and haematocrit in the definition of anaemia," *Tropical Medicine and International Health*, vol. 11, no. 8, pp. 1295–1302, Aug. 2006, doi: 10.1111/j.13653156.2006.01679.x.

[3] K. S. Oman, "Use of hematocrit changes as an indicator of blood loss in adult trauma patients who receive intravenous fluids," *Journal of Emergency Nursing,* vol. 21, no. 5, pp. 395–400,

Oct. 1995, doi: 10.1016/S0099-1767(05)80104-7.

[4] S. Kishimoto et al., "Hematocrit, hemoglobin and red blood cells are associated with vascular function and vascular structure in men," *Scientific Report*, vol. 10, no. 1, Jul. 2020, Art. no. 11467, doi: 10.1038/s41598-020-68319-1.

[5] Y. Z. Jin et al., "Relationship between hematocrit level and cardiovascular risk factors in a community-based population," *Journal of Clinical Laboratory Analysis*, vol. 29, no. 4, pp. 289–293, Jul. 2015, doi: 10.1002/jcla.21767.

[6] A. Chojecki et al., "Hematocrit control and thrombotic risk in patients with polycythemia vera treated with ruxolitinib in clinical practice," *Annals of Hematology*, vol. 103, no. 8, pp. 2837–2843, Aug. 2024, doi: 10.1007/s00277-024-05735-7.

[7] J. L. Spivak, "Polycythemia vera, the hematocrit, and blood-volume physiology," *The New England Journal of Medicine*, vol. 368, no. 1, pp. 76–78, Jan. 2013, doi: 10.1056/NEJMe1213283.

[8] C. Pellegrino, E. F. Stone, C. G. Valentini, and L. Teofili, "Fetal red blood cells: A comprehensive review of biological properties and implications for neonatal transfusion," *Cells*, vol. 13, no. 22, Nov. 2024, Art. no. 1843, doi: 10.3390/cells13221843.

[9] *Procedure for Determining Packed Cell Volume by Microhematocrit Method; Approved Standard-Third Edition*, NCCLS H7-A3, 2000.

[10] C. R. Flor, A. D. O. Baldoni, S. D. O. G. Mateos, E. C. Sabino, and C. D. L. Oliveira, "Comparison of two methods of capillary sampling in blood pre-donation anemia screening in Brazil," *Hematology Reports*, vol. 15, no. 2, pp. 298–304, Apr. 2023, doi: 10.3390/hematolrep15020030.

[11] World Health Organization (WHO), *Iron Deficiency Anemia: Assessment, Prevention and Control; A Guide for Program Managers*. USA: WHO, Jan. 2001.

[12] C. M. Chaparro and P. S. Suchdev, "Anemia epidemiology, pathophysiology, and etiology in low- and middle-income countries," *Annuals of the New York Academy of Sciences*, vol. 1450, no. 1, pp. 15–31, Aug. 2019, doi: 10.1111/nyas.14092.

[13] World Health Organization (WHO), *Anemia*. USA: WHO, 2025.

[14] W. M. Gardner and GBD 2021 Anaemia Collaborators, "Prevalence, years lived with disability, and trends in anaemia burden by severity and cause, 1990–2021: findings from the Global Burden of Disease Study 2021," *The Lancet Haematology*, vol. 10, no. 9, pp. e713–e734, Sep. 2023, doi: 10.1016/S23523026(23)00160-6.

[15] J. Sun, H. Wu, M. Zhao, C. G. Magnussen, and B. Xi, "Prevalence and changes of anemia among young children and women in 47 low- and middle-income countries," *EClinical Medicine*, vol. 41, Nov. 2021, Art. no. 101136, doi: 10.1016/j.eclinm. 2021.101136.

[16] C. Moscheo, M. Licciardello, P. Samperi, M. L. Spina, A. D. Cataldo, and G. Russo, "New insights into iron deficiency anemia in children: A practical review," *Metabolites*, vol. 12, no. 4, Mar. 2022, Art. no. 289, doi: 10.3390/metabo12040289.

[17] A. Z. Alem et al., "Prevalence and factors associated with anemia in women of reproductive age across low- and middle-income countries based on national data," *Scientific Reports*, vol. 13, Nov. 2023, Art. no. 20335, doi: 10.1038/s41598-023-46739-z.

[18] Geneva World Health Organization (WHO) and Centers for Disease Control and Prevention Atlanta (CDC), *Worldwide prevalence of anaemia 1993–2005: WHO Global Database on Anaemia 2008*. USA: WHO&CDC, 2008, pp. 97–100.

[19] N. J. Kassebaum, and GBD 2013 Anemia Collaborators, "The global burden of anemia," *Hematology Oncology Clinics of North America*, vol. 30, no. 2, pp. 247–308, Apr. 2016, doi: 10.1016/j.hoc.2015.11.002.

[20] G. Wennecke. "*Hematocrit-a review of different analytical method*." acutecaretesting.org. Accessed: Jul. 9, 2025. [Online.] Available: https://acutecaretesting.org/en/articles/hematocrit--a-review-of-different-analytical-methods.

[21] J. N. Kuo and B. S. Li, "Lab-on-cd microfluidic platform for rapid separation and mixing of plasma from whole blood," *Biomedical Microdevices*, vol. 16, no. 4, pp. 549–558, Mar. 2014, doi: 10.1007/s10544-014-9857-1.

[22] S. A. Mateen and K. S. Bhole, "A review on microfluidic devices for separation of blood constituents," *IOP Conference Series: Materials Science and Engineering*, vol. 810, no. 1, 2020, Art. no. 012024, doi: 10.1088/1757-899X/810/1/012024.

[23] Y. Shi et al., "A lab-on-disc centrifugal microfluidic system for ultraprecise plasma

separation," *Electrophoresis*, vol. 43, no. 21–22, pp. 2250–2259, Mar. 2022, doi: 10.1002/elps.202100359.

[24] R. Khodadadi, E. Pishbin, M. Eghbal, and K. Abrinia, "Real-time monitoring and actuation of a hybrid siphon valve for hematocrit-independent plasma separation from whole blood," *Analyst*, vol. 148, no. 21, pp. 5456–5468. Sep. 2023, doi: 10.1039/D3AN00862B.

[25] R. Khodadadi et al., "An integrated centrifugal microfluidic strategy for point-of-care complete blood counting." *Biosensors and Bioelectronics*, vol. 245, no. 1, Feb. 2024, Art. no. 115789, doi: 10.1016/j.bios.2023.115789.

[26] B. L. Thompson et al., "Hematocrit analysis through the use of an inexpensive centrifugal polyester-toner device with finger-to-chip blood loading capability," *Analytica Chimica Acta*, vol. 924, no. 14, pp. 1–8, Jun. 2016, doi: 10.1016/j.aca.2016.04.028.

[27] L. Riegger et al., "Single-step centrifugal hematocrit determination on a 10-$ processing device" *Biomedical Microdevices*, vol. 9, pp. 795–799, May 2007, doi: 10.1007/ s10544-007-9091-1.

[28] E. Pishbin, M. Navidbakhsh, and M. Eghbal, "A centrifugal microfluidic platform for determination of blood hematocrit level," in *2015 22nd Iranian Conference on Biomedical Engineering (ICBME)*, 2015, pp. 60–64, doi: 10.1109/ ICBME.2015. 7404117.

[29] C. Oksuz, C. Bicmen, and H.C. Tekin, "Dynamic fluidic manipulation in microfluidic chips with dead-end channels through spinning: the spinochip technology for hematocrit measurement, white blood cell counting and plasma separation," *Lab on a Chip*, vol. 25, no. 8, pp. 1926–1937, 2025, doi: 10.1039/D4LC 00979G.

[30] S. Rattanavarin et al., "Centrifugal microfluidic based painless blood sample collection for hematocrit measurement," in *2023 15th Biomedical Engineering International Conference (BMEiCON)*, 2023, pp. 1–5, doi: 10.1109/BMEiCON60347.2023. 10322045.

[31] K. J. Dziedzic, G. Zurawska, K. Banys, and J. Morozowska, "The impact of needle diameter and penetration depth of safety lancets on blood volume and pain perception in 300 volunteers: A randomized controlled trial," *Journal of Medical Laboratory and Diagnosis*, vol. 10, no. 1, pp. 1–12, Jan. 2019, doi: 10.5897/JMLD2018.0146.

[32] G. B. Abadi and M. Bahrami, "A general form of capillary rise equation in micro-grooves," *Scientific Reports*, vol. 10, no 1, Nov. 2020, Art. no. 19709, doi: 10.1038/s41598-020-76682-2.

[33] S. Sichamnan and A. Rodbumrung, "Effects of parameters on heat transfer characteristics of a rectangular cross-section heat pipe with mesh wick," *Applied Science and Engineering Progress*, vol. 15, no. 4, 2022, Art. no. 5628, doi: 10.14416/j.asep.2021.11.010.

[34] A. I. Shalaby, *Fluid Mechanics for Civil and Environmental Engineers*, Boca Raton, FL: CRC Press, 2018.

[35] S. S. Yadav, B. S. Sikarwar, P. Ranjan, R. Janardhanan, and A. Goyal, "Surface tension measurement of normal human blood samples by pendant drop method," *Journal of Medical Engineering & Technology*, vol. 44, no. 5, pp. 227–236, Jul. 2020, doi: 10.1080/03091902. 2020.1770348.

[36] J. D. Cutnell and K.W. Johnson, *Physics*, 4th ed. New York: Wiley, 1998, pp. 307–345.

[37] J. L. G. Cordero, L. M. Barrett, R. O'Kennedy, A. J. Ricco, "Microfluidic sedimentation cytometer for milk quality and bovine mastitis monitoring," *Biomedical Microdevices*, vol. 12, pp. 1051–1059, Aug. 2010, doi: 10.1007/s10544-010-9459-5.

[38] *Sample Size Calculator*, Statulator.com, 2025.

[39] *Sample Size Calculators; for designing clinical research*, Clinical and Translational Science Institute (UCSF), 2025.

[40] *EFLM biological variation database*, European Federation of Clinical Chemistry and Laboratory Medicine (EFLM), 2004.

[41] *2025 CLIA acceptance limits for proficiency testing*, WESTGARD QC, 2025.

[42] P. Wongkrajang, N. Opartkiattikul, W. Chinswangwatanakul, and S. Areewatana, "Accuracy and precision evaluation of Thai plastic microhematocrit tubes: The first product from Thailand," *The Journal of the Medical Association of Thailand*, vol. 95, no. 6, pp. 805–815, Jun. 2012.

[43] A. Dash, M. Mukhopadhyay, J. Shaw, M. Bhattacharya, and S. DasGupta, "Rapid hematocrit estimation using a fold-crease induced fast flowing paper sensor," *Sensors and Actuators B: Chemical*. vol. 418, Nov. 2024, Art. no. 136177, doi: 10.1016/j.snb.2024.136177.

[44] U. Pithanthanakul, V. Rungsardthong, and Y. Ding, "Surface and adhesion properties of a

softener containing fragrances microencapsulated with poly (methyl methacrylate) on cotton, polyester, and a mixture of cotton and polyester fabrics." *Applied Science and Engineering Progress*, vol. 17, no. 1, 2024, Art. no. 6846, doi: 10.14416/j.asep.2023.05.001.